

The Introduction of the Mean Field Approximation to Psychology: Combining Dynamical Systems Theory and Network Theory in Major Depressive Disorder

Jolanda J. Kossakowski^{1*}, Marijke C. M. Gordijn², Harriëtte Riese³ & Lourens J. Waldorp¹

*Correspondance: Jolanda J. Kossakowski
J.J.Kossakowski@uva.nl

¹Department of Psychology
University of Amsterdam
Nieuwe Achtergracht 129-B
1018 XE Amsterdam, The Netherlands

²Department of Chronobiology
GeLifes, University of Groningen
Groningen, The Netherlands

³Interdisciplinary Center Psychopathology and Emotion regulation
Department of Psychiatry
University Medical Center Groningen
University of Groningen, Groningen, The Netherlands

Abstract

Mental disorders like major depressive disorder can be seen as complex dynamical systems. We build on previous work using networks and dynamical systems theory in psychopathology, to investigate the dynamic behaviour of individuals to see whether or not they are at risk for a transition to another mood state. Here, we introduce a mean field approximation to a binomial process, where we reduce a dynamic multidimensional system (stochastic cellular automaton) to a one-dimensional system to analyse the dynamics. Using maximum likelihood estimation, we can estimate the parameter of interest which, in combination with a bifurcation diagram, reflects the risk that someone has to transition to another mood state. After validating the proposed method with simulated data, we apply this method to two empirical examples, where we show its use in a clinical sample consisting of patients diagnosed with major depressive disorder, and a general population sample. Results showed that the majority of the clinical sample was categorized as having an increased risk for a phase transition, while the majority of the general population sample did not have an increased risk. We conclude that the mean field approximation has great potential in assessing the risk for a transition between mood states. With some extensions it could, in the future, aid clinical therapists in the treatment of depressed patients.

Introduction

Major depressive disorder (MDD) is unfortunately not that uncommon: around 350 million people around the globe suffer from MDD (World Health Organization, 2012). While many studies have been conducted in the treatment of MDD, it remains unclear why certain people develop MDD and others do not; we do not know the exact circumstances of the person and its environment that may lead to MDD. There is some empirical evidence that people experience discrete mood states (Hosenfeld et al., 2015). This has led to the hypothesis that mood changes or (sudden) transitions to MDD may be related to dynamical systems theory (van de Leemput et al., 2014; Cramer et al., 2016; Wichers, Groot, Psychosystems, ESM Group, & ESW Group, 2016). In this paper, we build on these ideas to assess the risk of a person to develop MDD and embed such assessments more thoroughly in dynamical systems theory and network theory in order to obtain a reasonable explanation of transitions to MDD.

Recently, the idea has been put forward that mental disorders, like MDD, can be considered as a system of interacting variables (Borsboom, Cramer, Schmittmann, Epskamp, & Waldorp, 2011; Guloksuz, Pries, & Van Os, 2017; Cramer et al., 2016; Kossakowski & Cramer, 2018). Aspects of MDD, like loss of energy or feelings of worthlessness, can be seen as nodes in a network that interact, and thereby influence, themselves at later times and other symptoms of MDD (Cramer et al., 2012). This system of interacting emotions may change over time, making the system dynamic (Gulyás, Kampis, & Legendi, 2013): the influence of sleep deprivation on feelings of worthlessness may grow over time, as an individual is feeling more and more depressed. We can measure these changes by means of the Experience Sampling Method (ESM; Csikszentmihalyi & Larson, 1987), where individual daily life experiences can be measured several times a day for an extended period of time. At some point in time, when the system has surpassed some critical point (Scheffer et al., 2014), a discontinuous, transition is made from a stable and healthy phase to a stable and depressed phase. These sudden jumps, called *phase transitions* (Kuznetsov, 2013), are central to complex dynamical systems, and are subject of the risk assessment that we will undertake in the present paper.

Attempts to anticipate a phase transition are often approached by so-called early-warning signals obtained from time series (Kossakowski & Cramer, 2018). Dynamical systems leave ‘breadcrumbs’ behind in the time series that hint towards a phase transition. These breadcrumbs are called *early-warning signals* and occur before the phase transition, and after *critical slowing down*, an increase in the correlation of the time series with itself, representing the idea that it becomes more difficult to return to the original ‘good’ equilibrium state (Scheffer et al., 2014). Recently, it has been empirically shown that critical slowing down actually occurs, prior to the phase transition (van de Leemput et al., 2014; Wichers et al., 2016). While critical slowing down is an important line of research, it is difficult to analyse critical slowing down in a system that has more than a handful of variables.

In this study we take a different approach and try to assess the risk of possible (sudden) changes in mood. We extend the work of Hosenfeld et al. (2015), which uses a statistical measure to determine whether there is one or two stable mood states. The statistical measure, called the *bimodality coefficient* (BC), simply considers the distribution of the time series and determines whether there is evidence for one or two stable states. Here we extend this idea to embed it more concretely into network theory. We will simplify the system by reducing the network to a

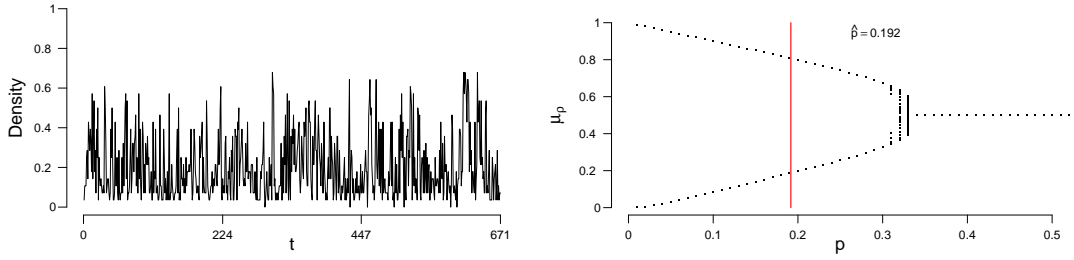


Figure 1. : The evolution of the percentage of active nodes for each time point (left figure), and the accompanying bifurcation diagram (right figure). The red line in the bifurcation diagram in the lower figures indicates the estimation of p .

single dynamic equation (given certain assumptions) and characterising the possible states of this reduced system. We then have a process that may be an accurate description of what is going on with the changes in symptoms over time. We can, in turn, analyse these changes analytically and through simulations. We assume (intuitively) that the nodes in the network function roughly in the same manner and that each of the nodes affects the others in a similar way. The assumptions lead to a so-called mean field model. Using these assumptions, our focus becomes the proportion of active emotions in the system, which now forms a sequence of states ranging from 0 to 1. Since this sequence of states only depend on the proportion of active emotions at the previous time point, we obtain what is called a Markov chain and we can estimate the parameters by maximum likelihood in a straight forward manner. Using this dynamical system allows us to determine whether for a person it is possible that a phase transition may occur or not.

As an example, we consider a time series of the proportion of active emotions for a single subject, shown in Figure 1 (left). We identify the possible states of this person with respect to the network of emotions, depending on the parameter of the process we assume underlying the observations. For this process we can obtain a so-called bifurcation plot (Figure 1, right). The bifurcation plot shows the possible (likely) states for this person given a value on the probability p of emotions changing from inactive to active. We assess from the time series of this person the parameters of our model and obtain an estimate of where in the bifurcation plot this person is (red line in Figure 1, right). If the probability p is in the range of $[0.34, 0.50]$ then this person will remain stable. If the probability is lower than approximately 0.34, then there are two stable states, one with a high proportion of active emotions and one with a low proportion of active emotions. The estimate of the probability p for this person is 0.192 (the red vertical line in the right part of Figure 1) and so is classified as someone who may show a (sudden) increase in the proportion of active emotions and thereby experience an episode of depression. And indeed, for this subject we know (from external evidence) that a depressive episode had taken place after the time series that we used to determine the state of the person (see Wichers et al., 2016; Kossakowski, Groot, Haslbeck, Borsboom, & Wichers, 2017).

This paper is set up as follows. First, we explain the theory of the mean field approximation and the proposed method. Then we present a simulation study to show that the proposed

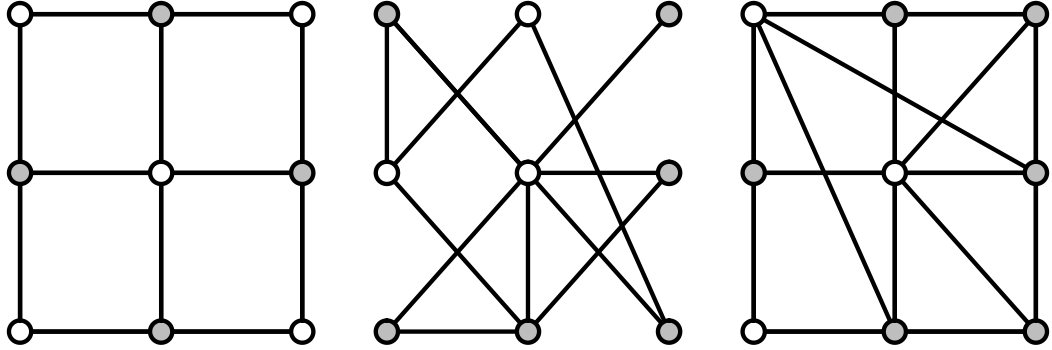


Figure 2. : Visualization of a grid structure (left figure), a random graph structure (middle figure), and a small-world structure (right figure). Grey nodes indicate the neighbours of the middle node in each graph.

method works well. And finally we apply the method to a data set to show how the proposed method works in practice.

Stochastic cellular automata

To model the interacting emotions we use a particular kind of structure, a stochastic cellular automaton. Such automata are particular dynamical systems that show typical behaviour of stable and bistable behaviour depending on the settings (Kozma, Puljic, Balister, Bollobás, & Freeman, 2004; Balister, Bollobás, & Kozma, 2006), which is what we assume to hold for MDD. A cellular automaton (CA) is a dynamical system where nodes are arranged in a fixed and finite grid, and where connected nodes determine the state of a node at each subsequent time point (Wolfram, 1984; Sarkar, 2000). A node y that is directly connected to node x is called a neighbour. A grid is a graph $G_{\text{grid}}(n, \Gamma)$ with n nodes in the set $V = \{1, 2, \dots, n\}$ where each node x has the same number of neighbours in its neighbourhood $\Gamma = \{y \in V : y \text{ is connected to } x\} \cup \{x\}$ including itself. To ensure that all nodes have exactly the same number of neighbours, we impose the boundary condition such that a node at the boundary is connected to a node on the opposite end, making it a torus. An example of such a grid is shown in Figure 2 (left), where the center node is directly connected to its four neighbours, marked in grey. We consider elementary CAs where each node can be in either of two states: ‘active’ (coded by 1) or ‘inactive’ (coded by 0). In a CA a deterministic, local update rule ϕ determines the state of each node at the next time step based on which nodes are active in the neighbourhood of x . An example of this is the majority rule, where each node becomes 1 whenever more than half of the neighbours of x at the previous time step are active, and 0 otherwise. Although many other update rules are possible, we will focus on this particular rule in the present study. Repeated application of the update rule ϕ results in a vector of 0s and 1s called an orbit: At any time point t the orbit $\phi^t(x) = \phi(\phi \cdots \phi(x))$, such that the same local rule is applied t times.

In a stochastic cellular automaton (SCA), a probability is introduced to model uncer-

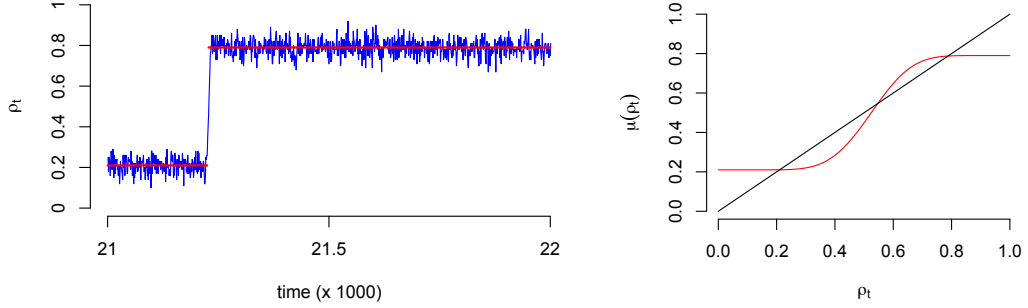


Figure 3. : Example of a stochastic cellular automata process that includes a phase transition (left). Example of the corresponding mean field function. The red line indicates the expectation of equation (3) divided by the number of nodes.

tainty, based on the number of active neighbours. In our application to psychopathology, this uncertainty is required because we cannot predict the behaviour of the emotions in our network exactly, and because we know that exogenous events influence these emotions which we cannot measure. The probability $0 \leq p \leq 1$ determines whether or not a node becomes active at time point $t + 1$. The majority rule with the probabilistic update used in this study is

$$\xi_{|\Gamma|}(r) = \begin{cases} p & \text{if } r \leq |\Gamma|/2 \\ 1-p & \text{if } r > |\Gamma|/2 \end{cases} \quad (1)$$

where $|\Gamma|$ is the size of the neighbourhood and r the number of active neighbours. Because $\xi_{|\Gamma|}$ is dependent on the behaviour of the majority of a node's neighbourhood, this update rule is also called the *majority rule*. In this SCA each node $x \in V$ is then updated according to the majority rule; all nodes are updated simultaneously (synchronous updating). The result for each node is a sequence of 0s and 1s. For all $n = |V|$ nodes we have the orbits $(\phi^t(x), t \geq 0)$, which are vectors of length T for the total duration. We average over all nodes in the grid at each time point t , $\rho_t = \frac{1}{n} \sum_{x \in V} \phi^t(x)$, which is called the *density*. An example of this is shown in Figure 1 (left panel).

Mean field approximation

To infer from an SCA the characteristics of what the system will do in the long run can be rather difficult (Lebowitz, Maes, & Speer, 1990). We need to simplify the SCA in order to make it possible to derive the characteristics of the SCA. Here we use the assumption of uniformity that allows us to reduce the n -dimensional system to a one-dimensional system. In the grid (Figure 2, left) it is easily seen that each node is similar to any other node since each node has the same number of neighbours, and becomes active or inactive in the same way by means the majority rule that is based on the number of active neighbours. This allows us to simplify an

SCA to a single discrete time dynamical system, as in Kozma, Puljic, Balister, Bollobás, and Freeman (2005) and Balister et al. (2006). Here we explain in general terms how we obtain the mean field approximation, but for more details see Waldorp and Kossakowski (2018).

In the *mean field* approximation we make use of the uniformity of the nodes in a grid. Each node changes value from 0 to 1 or vice versa based on the number of active nodes in its neighbourhood $|\Gamma|$ with probability $1 - p$ or p , respectively, according to the majority rule. In a grid each node has exactly the same number of neighbours and so the probability of a node changing value depends on the properties of the grid and not on the local activity. Therefore, as shown in Kozma et al. (2005); Balister et al. (2006), we obtain that at time point $t + 1$ the number of active nodes in the grid $n\rho_{t+1}$, which is a binomial probability with success probability ρ_t of the previous time point t . The number of draws in the binomial probability is determined by the size of the neighbourhood $|\Gamma|$. The majority rule in (1) determines for which number of active nodes we obtain p up until $r \leq \lfloor |\Gamma|/2 \rfloor$, or $1 - p$ otherwise. To define the probability of the number of neighbours that are 1, let

$$\pi_{|\Gamma|/2}(\rho_t) = \sum_{r=0}^{\lfloor |\Gamma|/2 \rfloor} \binom{|\Gamma|}{r} \rho_t^r (1 - \rho_t)^{|\Gamma| - r} \quad (2)$$

where $\lfloor a \rfloor$ is the integer part of a . Then, as Balister et al. (2006) showed and restated in Waldorp and Kossakowski (2018), we obtain the probability of a node being active given the majority rule (1)

$$p_{\text{grid}}(\rho_t) = p\pi_{|\Gamma|/2}(\rho_t) + (1 - p)(1 - \pi_{|\Gamma|/2}(\rho_t)) \quad (3)$$

It follows that the transition probability that the number of active nodes $n\rho_{t+1} = v$, given that at t is $n\rho_t = u$ in the graph G_{grid} , is

$$\mathbb{P}(n\rho_{t+1} = v \mid n\rho_t = u) = \binom{n}{r} p_{\text{grid}}(u/n)^r (1 - p_{\text{grid}}(u/n))^{n-r} \quad (4)$$

So, we know how in a grid with n nodes the proportion of active nodes changes from time point t to time point $t + 1$, for any t . The mean field approximation uses the mean of this binomial process and divides by n to obtain the proportion, which is $\mu_{\text{grid}} = p_{\text{grid}}$. We know that the fluctuations around the mean are small (depending on the standard deviation and size of the grid, see Waldorp and Kossakowski (2018)), so the mean is a good approximation of the process itself.

As an illustration of the binomial process, in the left panel of Figure 3 we see a typical SCA process where it is clear that the fluctuations are around a particular mean (0.2) for time points before $t = 21000$ approximately. After this point (tipping point) the fluctuations revolve around another mean (0.8) with a higher proportion of emotions. In the right panel of Figure 3 we see a plot of the expectation of the process, which is the mean field that predicts the values at which the mean of the process will be eventually. It is this mean function that we will use to represent the process and the network that evolves over time.

We now regard the mean field $\mu_{\text{grid}} = p_{\text{grid}}$ as the dynamical system that is a representation of the network. This dynamical system evolves by repeated application of p_{grid} to its previous

result. We analyse the dynamical properties of p_{grid} by considering a so-called bifurcation plot. Plugging in different values for p in the majority rule, in the interval $(0, 0.5]$, we obtain a *bifurcation diagram*, of which examples are shown in Figure 1. In a bifurcation diagram the repeated application of p_{grid} is applied to updated values of ρ_t such that the last section of the orbit is displayed where the process is in equilibrium (stable if stable fixed points exist; Hirsch, Smale, & Devaney, 2012). Such diagrams show what kind of behaviour can be expected to be generated by the process. Here we see that there are two kinds of situations: (a) a stable situation when p is in the interval $(0.34, 0.50]$, where irrespective of the starting point, the process ends up at that stable fixed point, and (b) a bistable situation when p is in $[0, 0.34]$ where the process could (suddenly) switch between states (phase transition) to a low or high density. The parameter value p at which the process changes from a stable to a bistable situation is called the critical point. In Figure 1 the critical point lies at $p \approx 0.34$; the parameter area $0 < p \leq 0.34$ is bimodal where phase transitions can occur, whereas the parameter area $0.34 < p < 0.50$ represents a unimodal area where the mean field is stable.

The probability for the mean field in (3) is designed for a torus with a fixed neighbourhood size $|\Gamma|$. In the context of psychology and psychopathology, it is hard to come up with a graph representing the interactions between variables, that would take the form of a grid (torus). We therefore also looked at the mean field approximation for a *random graph* and a *small-world graph*.

A random graph $G_{\text{rg}}(n, p_e)$ is a graph structure with n nodes and a (constant) probability p_e for an edge to be present in the graph (Bollobás, 2001; Durett, 2007). In the mean field approximation of a random graph, the neighbourhood size $|\Gamma|$ is a random variable that is maximally $n - 1$. Let $v = \lfloor p_e(n - 1) \rfloor$ be the integer part of the expected number of neighbours with probability of an edge p_e . The difference with the probability on the grid is in the size of the neighbourhood in the function π (see Figure 2), here for the random graph G_{rg} it is v and in the grid G_{grid} it is $\lfloor |\Gamma|/2 \rfloor$, where $|\Gamma|$ often is 5 in a two-dimensional grid (4 neighbours and the node itself at the previous time point). The probability for a node to become active given the graph's density at time point t and the edge probability then becomes (Waldorp & Kossakowski, 2018).

$$p_{\text{grid}}^v(\rho_t) = p\pi_v(\rho_t) + (1 - p)(1 - \pi_v(\rho_t)) \quad (5)$$

It can be shown that this approximation for the probability of a node being active is accurate (see Waldorp & Kossakowski, 2018).

A small-world graph is in between a grid and a random graph where, compared to a random graph, the average clustering is high and the average path length is low (Watts & Strogatz, 1998). A modified version of the small world is the Newman-Watts (NW) small-world (Newman & Watts, 1999). In the NW small-world $G_{\text{sw}}(n, \Gamma, p_w)$ the n nodes each have a neighbourhood $|\Gamma|$ as in the grid and edges are added to the graph following a (constant) wiring probability p_w (Newman & Watts, 1999). We can then split up the probability in a part associated with the grid and a part associated with the random graph. The part for the grid is adjusted such that it corresponds to no other edges being present, i.e., we obtain $p_{\text{grid}}^{\text{sw}} = p_{\text{grid}}(1 - p_w)^{n - |\Gamma|}$. Then for the random part we obtain exactly those possible edges that could be included in the neighbourhood out of the remaining $n - |\Gamma|$ nodes that are possibly active, i.e., $p_{\text{grid}, \Gamma}^v$, which denotes the

probability as in (5) but with $p_{\text{grid},\Gamma}^v$ starting at $|\Gamma| + 1$ instead of 0. Then the probability for a node to become active given the graph's density at time point t and the wiring probability in the small-world graph G_{sw} is

$$p_{\text{sw}}(\rho_t) = \frac{|\Gamma|}{n} p_{\text{grid}}(1 - p_w)^{n-|\Gamma|} + \frac{n - |\Gamma|}{n} p_{\text{grid},\Gamma}^v \quad (6)$$

The small-world probability is therefore a combination of the probability on the grid and on a random graph, proportionately weighted.

Estimation of probability p and graph parameters

The mean field approximation assumes that each neighbourhood $|\Gamma(x)|$ is equal for all $x \in V$. In a random and small-world graph, this assumption is violated as edges have a constant probability either to be drawn (random graph; p_e) or rewired (small world graph; p_w). Waldorp and Kossakowski (2018) investigated the effect of violating this assumption by performing a simulation study, in which the accuracy of the mean field approximation in these different graphs is evaluated. They showed that the mean field approximation accurately estimates the density for different graph structures.

Here, our objective is to determine from a time series the density of a graph obtained from data, an estimate to determine whether or not this person is at risk of phase transitions to a different state, possibly MDD. One way of obtaining such a risk assessment is to determine where in a bifurcation diagram a person is located with respect to the parameter p in the majority rule; is this in the stable area, where no transition can occur, or is it in the bistable area where a transition can occur. In order to do this, we need to estimate the parameter p of the majority rule. Here we use maximum likelihood (ML) to obtain an estimate of p (Rajarshi, 2012).

If we take a closer look at equations (2) and (3), it can be noticed that all parameters are known prior to the analysis, with the exception of the probability parameter p . To obtain the probability parameter p , we can estimate it from the data using ML estimation. We then obtain the maximum of the log-likelihood for the majority rule parameter p . We write the transition probability in going from state u to state v (number of active nodes) in (4) from t to $t + 1$ as $\mathbb{P}(n\rho_{t+1} = v | n\rho_t = u) = p_{u,v_{t+1}}$. The log of the joint probability function (loglikelihood) for the number of active nodes is then

$$\log \mathbb{P}(n\rho_t, t \geq 0) = \sum_{t=0}^{T-1} \log p_{u_t, v_{t+1}} \quad (7)$$

We recognise in the SCA that we can relatively easily find the transition probability to go from u to v active nodes by the fact that we have for each of the graphs G_{grid} , G_{rg} , and G_{sw} a binomial process with a probability of success particular to each type of graph. And we obtain the transition probability in (4). The transition probabilities for the random graph G_{rg} and the small-world graph G_{sw} are similar except that we change the probability of success to p_{rg} or p_{sw} , respectively.

The process is ergodic whenever the probability p_{grid}^v is not in the basin of attraction of 0 and 1 (see Waldorp & Kossakowski, 2018). In those cases we could simplify expression (7) using only the transition probabilities that do not depend on time. In general, however, we do not know where the probabilities are, and so we do not assume ergodicity (and hence stationarity)

and so cannot simplify the log-likelihood to terms consisting only of the states and not on time (Fleming & Harrington, 1978). We maximise the log-likelihood function in (7) with respect to p to obtain its estimate from an empirical time series, making it possible to place that person on the bifurcation diagram and assess the risk of possible switching.

In both the random and small-world graph we have additional graph parameters: in the random graph we have the probability of an edge p_e , and in the small-world graph we have the probability of wiring p_w . Both parameters are obtained by maximising the log-likelihood with respect to p_e and p_w respectively.

Equations (3), (5) and (6) each show how we calculate the density in a grid, a random graph, or a small-world graph, respectively. One only needs to plug in a value for p (and the graph parameters p_e or p_w in the case of a random graph or a small-world graph, respectively) into the equation and let it run for some time t (often 1000 is enough), to find out at what density it will end up, or between which two values it may transition in the case of two stable states. By varying the value for p , one can create a bifurcation diagram, of which examples are shown in Figure 4. Each dot represents a separate run of the mean field equation.

Taking the upper figure of Figure 4 as an example, if we run equation (3) with $p = 0.1$, it can be seen that the binomial process ends up in either 0.1 or 0.9 approximately, and could switch between these states. Our mean field model says that if we estimate the parameter of a person at about 0.1, then this person is at risk of possible transitions between the two states, which could be related to a depressive episode. When we increase p to 0.3, the binomial process no longer has the possibility of a transition between states, but will remain around 0.5 approximately. The critical point, the point where the system changes from having two stable states to one stable state, differs depending on the size of the graph and the type of graph; for the random graph and the small-world graph the location of the critical point also depends on the graph parameters p_e or p_w , respectively, as seen in Figure 4. To summarize, in order to categorize individuals, we need to know what the individual's position is in its personalized mean field model.

Validation of probability p and graph parameters

Here, we determine whether the mean field approximation is able to correctly categorize data that was simulated by Waldorp and Kossakowski (2018). Waldorp and Kossakowski simulated 100 networks for each topology of a grid, a random graph, and a small-world graph. They varied the size of the network $n \in \{ 16, 25, 49, 100 \}$, the number of time points $T \in \{ 50, 100, 200, 500, 5000 \}$, and the probability $p \in \{ 0.1, 0.2, 0.3, 0.4, 0.5, 0.6, 0.7, 0.8, 0.9 \}$ (Equation 3). They also varied the probability for an edge in the random graph $p_e \in \{ 0.1, 0.2, 0.3, 0.4, 0.5, 0.6, 0.7, 0.8, 0.9 \}$ (Equation 5) and the probability for an edge to be rewired in the small-world graph $p_w \in \{ 0.1, 0.2, 0.3, 0.4, 0.5, 0.6, 0.7, 0.8, 0.9 \}$ (Equation 6). For $t = 0$, a random number of nodes was set to active by using the R package *IsingSampler* version 0.2 (Epskamp, 2015).

For each of the 100 simulation runs, we used the $t \times n$ set of active and inactive nodes to optimize p and the graph parameters p_e and p_w . All simulated data, figures, and the used R-code are publicly available at the open science framework (OSF; Kossakowski, 2018). For clarity of presentation, figures are only presented for $T = 500$, as results for $T = 50$ and $T = 100$ were nearly identical, or slightly worse. For each simulation run, we calculated the absolute

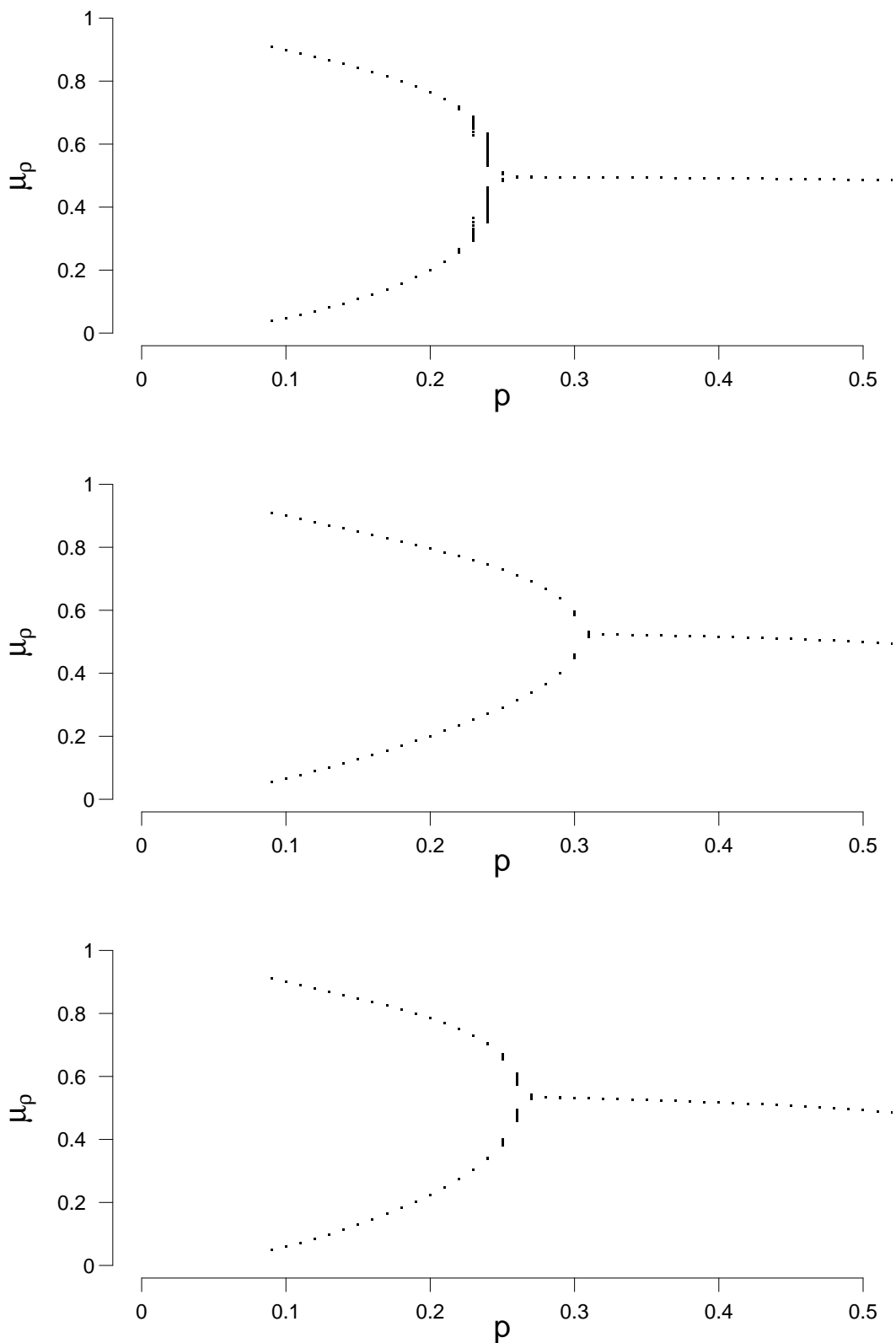


Figure 4. : Examples of bifurcation diagrams for a grid (top figure), a random graph (middle figure; $p_e = 0.1$) and a small-world graph (lower figure; $p_w = 0.1$).

difference between the value p , under which the data were simulated, and \hat{p} , which we estimated from the data. We denoted this difference by Δ_p , after which the mean absolute difference ($\bar{\Delta}_p$) is determined for each condition, which can be interpreted as an error rate. The lower this value, the closer the estimate \hat{p} is to the original value p . The same procedure was performed to determine the accuracy for graph parameters p_e ($\bar{\Delta}_{p_e}$) and p_w ($\bar{\Delta}_{p_w}$). Figure 5 shows a 2D and a 3D representation of the mean absolute difference between the true parameter p , and the estimated parameter \hat{p} . It can be seen that the error rate for p is low for all different network structures ($\bar{\Delta}_p = 0.04$ across all conditions). The only exception to this is in the case of the random graph, shown in the middle column of Figure 5, where the error rate $\bar{\Delta}_p$ increases at low values for p , and decreases as p increases.

The same conclusion cannot be drawn for graph parameters p_e and p_w , as seen in Figure 6. For a random graph, $\bar{\Delta}_{p_e}$ is high when p_e is low, and decreases as p_e is increased. This shows that graph parameter \hat{p}_e is most accurate when p_e is high. A possible explanation for this finding could be found in the connectedness of random graphs. When p_e is small, the probability that not all nodes are connected increases, resulting in isolated nodes. When we look at the minimum probability p_e , such that the graph is connected for different network sizes, we see that p_e must be at least 0.46 when the network size is 16, 0.31 when the network size is 25, 0.17 when the network size is 49 and 0.09 when the network size is 100. Thus, as p_e increases, the probability for the network to be connected increases, and as a result of this, the error $\bar{\Delta}_{p_e}$ decreases. The reverse is true for a small-world graph, where $\bar{\Delta}_{p_w}$ is high when p_w is high and p is low, and that it decreases when p_w also decreases. This shows that graph parameter \hat{p}_w is most accurate when p_w is low and when p is high.

In sum, the mean field approximation estimates p well from the data; the graph parameters p_e and p_w could not be estimated as accurately. For the random graph parameter p_e , this could potentially be solved by taking the ratio of edges present in the graph, and the total number edges possible in the graph. Alas, there is no similar solution for the small-world graph parameter p_w . In the application of the mean field approximation, we assume all graphs to be random graphs. As estimating p_e from the data and extracting it from the graph resulted in nearly identical results, we decided to use the former option.

Application to empirical time-series data

Here, we will demonstrate how the probability p of an emotion to be active is estimated from empirical data. In the following sections, we will show two empirical examples and demonstrate how the proposed method works in each of these examples. By showing the application of our proposed method on two different kinds of data, we aim to show how our proposed method works for different participants, and different types of data. The first example is a dataset of patients who were admitted as patients to a closed, psychiatric ward of an academic hospital (Gordijn, Beersma, Bouhuys, Reinink, & van den Hoofdakker, 1994; Gordijn, Beersma, Bouhuys, & van den Hoofdakker, 1998). The second example is a dataset of healthy participants who were originally recruited in a nation-wide study (van der Krieke et al., 2015).

The data in these examples are time-series data. When collecting these types of data, participants are asked to complete a questionnaire several times a day. These questionnaires often contain items regarding a participant's current mood state, but can also hold items regarding a

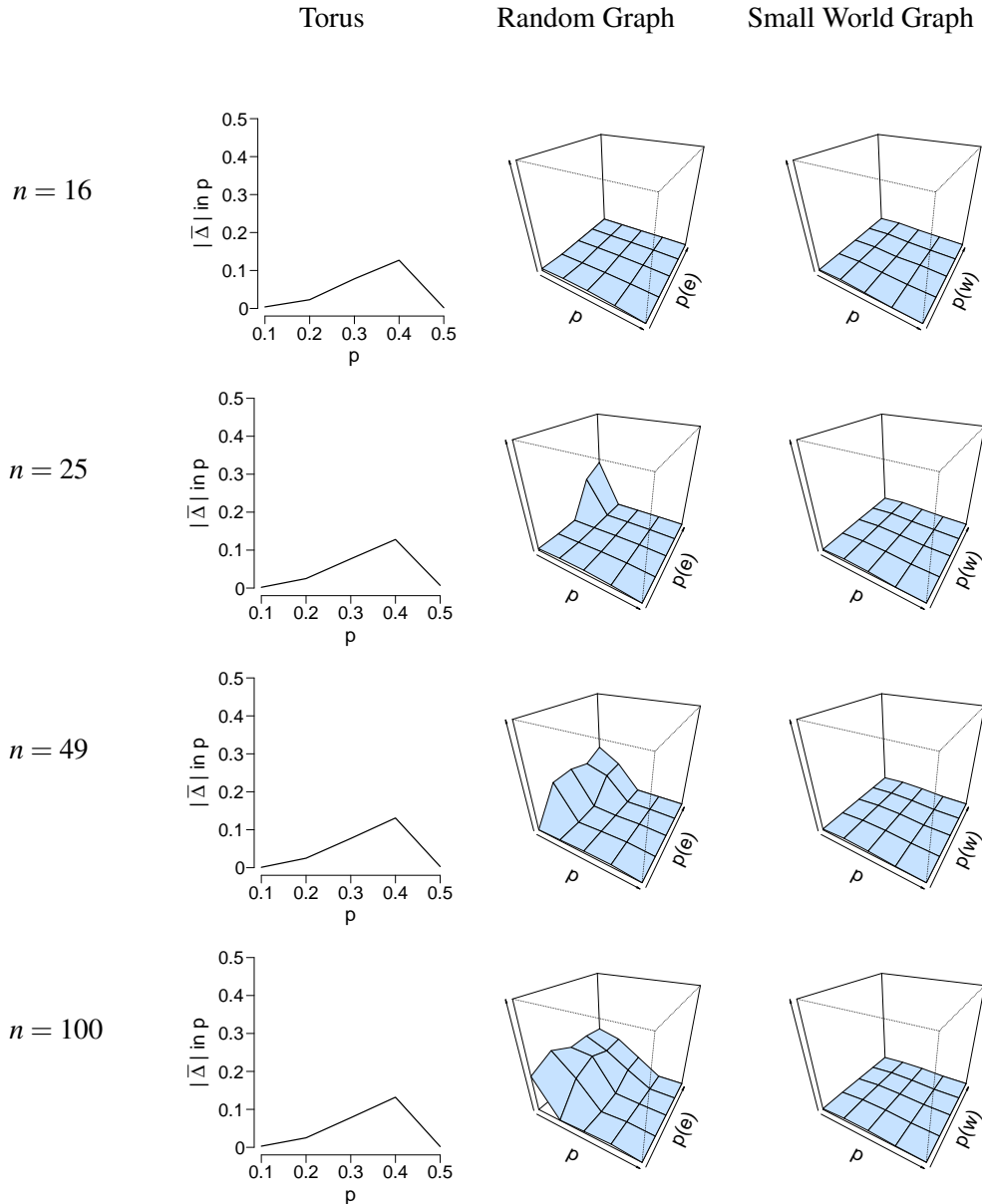


Figure 5. : Visualization of the mean absolute differences between p and \hat{p} . Mean absolute difference is shown for a torus (left column), a random graph (middle column), and a small world graph (right column). For the left column, the x-axis denotes the parameter p for which we simulated data, and the y-axis the mean absolute difference between p and \hat{p} . For the middle and right column, the x-axis denotes the parameter p for which we simulated data, the y-axis the graph parameter that was used to simulate data, and the z-axis the mean absolute difference between p and \hat{p} .

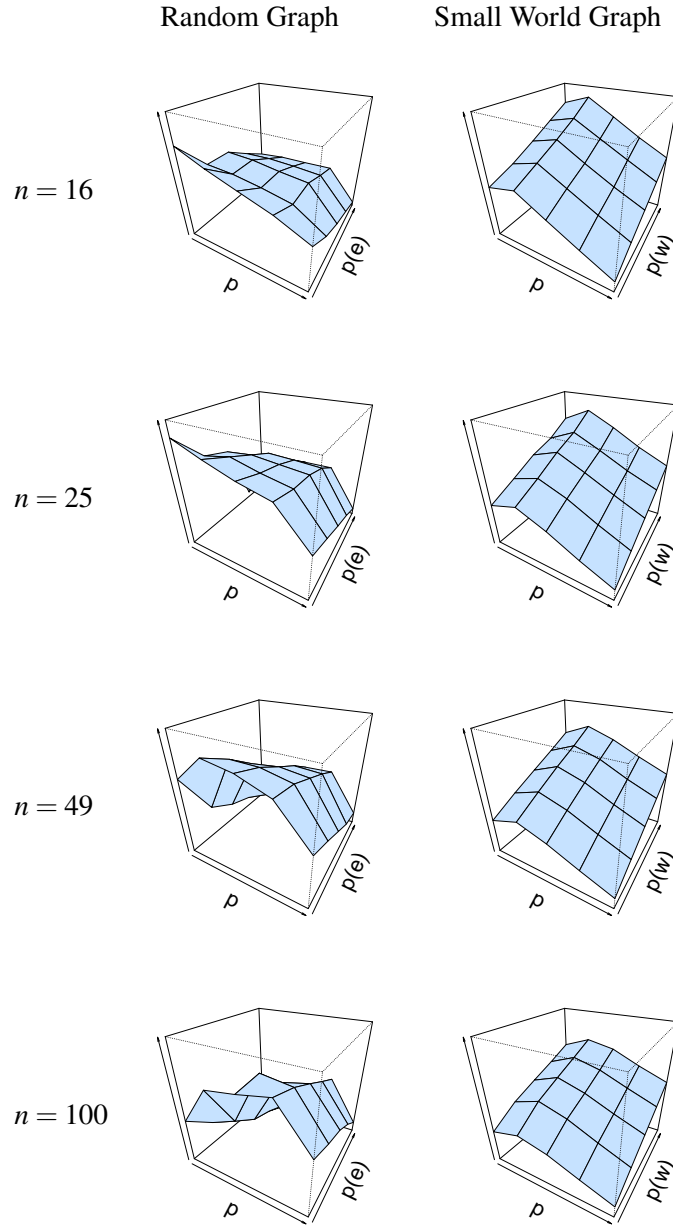


Figure 6. : Visualization of the mean absolute differences between p_e and \hat{p}_e and p_w and \hat{p}_w . Mean absolute difference is shown for a random graph (left column) and a small world graph (right column). The x-axis denotes the parameter p for which we simulated data, the y-axis the graph parameter that was used to simulate data, and the z-axis the mean absolute difference between p and \hat{p} .

participant's physical condition, for example. In both examples, participants received a 'beep' on fixed times during the day and were asked to complete the questionnaire. These beeps, in turn, correspond to the time points in time-series data. For example, when a participant completed twenty questionnaires, the data contains $t = 20$ time points. All analyses were performed using the R statistical software 3.4.4 (R Core Team, 2016).

Example 1: Clinical sample

This example involves a secondary analysis of data that were originally gathered for a study in patients diagnosed with MDD, who were admitted to a closed, psychiatric ward of an academic hospital (Gordijn et al., 1994, 1998). The data have been described in detail in previous papers (Gordijn et al., 1994, 1998). Participants in this study completed the Dutch version of the Adjective Mood Scale (AMS; von Zerssen, 1986) twice a day at fixed time points for a period of six weeks, resulting in a maximum of 84 measurements per participant. Participants had to indicate on this 28-item questionnaire which of two given emotions (or neither) corresponded most closely to the participant's emotion at that moment in time. A detailed description of the items of the AMS can be found in Table 1.

We dichotomized the data by collapsing the 'neither' condition with the positive mood state. We coded the positive mood state as '0' and the negative mood state as '1'. We also considered including the 'neither' condition with the negative mood state, but as these results were very similar to the ones we present, we left it out of this study. After dichotomizing the data, we replaced any missing measurement with the previous measurement. We also considered removing the missing measurements entirely, but as we found nearly identical results, we chose not to present these results.

A total of 82 participants were initially included in the study. Nineteen participants were excluded from the analyses due to a too low number of measurements (< 5), resulting in 63 participants that were included in the analyses. (Excluded participants (mean age = 46.89 years, SD = 15.60 years, 73.68% women) missed on average 42.36% of the measurements, and completed on average 48.21 measurements (SD = 35.34). These participants were admitted between 1988 and 1993, and were admitted on average for 205.47 days (SD = 138.63 days, min = 49 days, max = 536 days)). Included participants had a mean age of 48.68 (SD = 12.84 years) at the time of admission to the closed ward, with 71.14% women. These participants missed on average 9.62% of the measurements, and registered on average 84 measurements (SD = 0). Participants were admitted between 1988 and 1994, and were admitted on average for 186.45 days (SD = 121.86 days, min = 61 days, max = 572 days). Raw results from all analyses can be found online (Kossakowski, 2018).

Figure 7 shows the evolution of the density (left figure), a histogram of the density (middle figure), and the estimate of \hat{p} in the bifurcation diagram (right figure) of a single participant. Figures of all participants are available online. According to the mean field approximation 84.2% of the participants have an increased risk for a phase transition. This is not surprising given that the sample is from a population of patients on a psychiatric ward. To compare, we calculated the bimodality coefficient (BC), which uses a function of the skewness and kurtosis from the distribution of the time series of the proportion of symptoms (see Hosenfeld et al. (2015) for details). The BC obtains values between 0 and 1 and considers values > 0.55 to mean

Item	Item meaning (Dutch)	Item meaning (translation to English)
1	Ik voel me nu openhartig/geremd	I currently feel openly/inhibited*
2	Ik voel me nu welgemoed/droefgeestig	I currently feel a good mood/a bad mood*
3	Ik voel me nu inactief/bedrijvig	I currently feel passive/active
4	Ik voel me nu ziekelijk/kiplekker	I currently feel sickly/healthy
5	Ik voel me nu doelbewust/doelloos	I currently feel purposefully/aimlessly*
6	Ik voel me nu ernstig/geestig	I currently feel serious/humorous
7	Ik voel me nu fantasieeloos/fantasierijk	I currently feel unimaginative/imaginative
8	Ik voel me nu gevoelig/gevoelloos	I currently feel sensitive/numb*
9	Ik voel me nu pessimistisch/optimistisch	I currently feel pessimistic/optimistic
10	Ik voel me nu zorgeloos/tobberig	I currently feel carefree/worried*
11	Ik voel me nu gebroken/monter	I currently feel broken/cheerful
12	Ik voel me nu liefderijk/liefdeeloos	I currently feel lovingly/loveless*
13	Ik voel me nu schuldig/onschuldig	I currently feel guilty/innocent
14	Ik voel me nu uitgeput/uitgerust	I currently feel tired/rested
15	Ik voel me nu levensmoe/levenslustig	I currently feel life-tired/lively
16	Ik voel me nu goed/slecht	I currently feel good/bad*
17	Ik voel me nu vrolijk/treurig	I currently feel cheerful/tearful*
18	Ik voel me nu bemind/onbemind	I currently feel loved/unloved*
19	Ik voel me nu lui/actief	I currently feel lacking in energy/energetic
20	Ik voel me nu gesloten/open	I currently feel withdrawn/sociable
21	Ik voel me nu levendig/levenloos	I currently feel lively/sluggish*
22	Ik voel me nu temperamentvol/futloos	I currently feel temperamental/lifeless*
23	Ik voel me nu opletend/verstrooid	I currently feel watchful/absent*
24	Ik voel me nu wanhopig/hoopvol	I currently feel desperate/hopeful
25	Ik voel me nu tevreden/ontevreden	I currently feel satisfied/dissatisfied*
26	Ik voel me nu angstig/strijdlustig	I currently feel anxious/combative
27	Ik voel me nu krachtig/krachteloos	I currently feel powerful/powerless*
28	Ik voel me nu evenwichtig/gejaagd	I currently feel balanced/agitated*

Table 1:: Items of the Adjective Mood Scale (AMS) and their assigned labels.* Items that have a reversed response scale. The English translation may differ from the original AMS scale, as well as the order of the items.

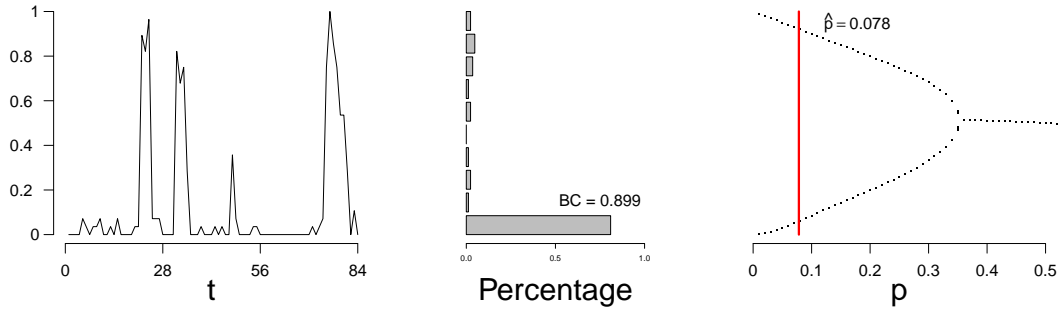


Figure 7. : Proportion of active symptoms (left) and bifurcation diagram (right) of one participant from the the Groningen data. BC = bimodality coefficient. Red line indicates the estimation of \hat{p} .

there is evidence for two states. The BC classified 57.9% of the cases as being bimodal. When we compare the results from the MFA to the BC, we see that the methods agree in 52.6%.

Example 2: General sample

Participants were originally recruited in a nation-wide study called HoeGekIsNL (in English: HowNutsAreTheDutch) and have been described in detail in a previous paper (van der Krieke et al., 2015). Participants in this study filled out a 43-item questionnaire that consisted of new items created for this study, and items from existing and validated questionnaires. Participants completed this questionnaire three times a day with a six-hour interval between the time points, for a period of 31 days, resulting in a maximum of 93 measurements per participant (van der Krieke et al., 2015).

From the original questionnaire, we selected items that pertained to mood states (21 items), appetite (one item) and laughter (one item), ending up with 23 items. Table 2 shows a detailed description of the included items. We recoded 10 positive items so that high scores indicate a more negative affect on all items. All included items were measured on a 0-100 scale. We dichotomized the data using a median split. We coded the all responses below the median as '0', and everything above the median as '1'. We also considered using a k-means clustering to dichotomize the data, but as these results were very similar to the results that we present, we chose not to include these results here. We replaced any missing measurements with the previous measurement. We also considered removing the missing measurements entirely, but as we found nearly identical results, we chose not to present these results.

A total of 974 participants participated in this study. We excluded 254 participants from the analyses due to a too low number of measurements (< 5), resulting in 720 participants that were included in the remainder of this section. (Excluded participants (mean age = 41.07 years, $SD = 13.47$ years, 83.5% women) missed on average 84% of the measurements, and completed an average of 3.03 measurements ($SD = 2.92$). Included participants had a mean age of 40.15 ($SD = 13.51$ years) at the start of the data collection, with 82.5% women. These participants missed on average 30.50% of the measurements and registered on average 93.39 measurements

Item	Item meaning
1	I feel relaxed
2	I feel gloomy
3	I feel energetic
4	I feel anxious
5	I feel enthusiastic
6	I feel nervous
7	I feel content
8	I feel irritable
9	I feel calm
10	I feel dull
11	I feel cheerful
12	I feel tired
13	I feel valued
14	I feel lonely
15	I feel I fall short
16	I feel confident
17	I worry a lot
18	I am easily distracted
19	I feel my life is worth living
20	I am unbalanced
21	I am in the here and now
22	My appetite is..
23	Since the last measurement I had a laugh

Table 2:: Items that were included in the analysis and their assigned labels.

(SD = 34.56). Raw results from all analyses can be found online (Kossakowski, 2018).

Figure 8 shows the evolution of the density (left figure), a histogram of the density (middle figure), and the estimate of \hat{p} in the bifurcation diagram (right figure) of a single participant. Figures of all participants are available online. According to the mean field approximation 22.4% of the participants have an increased risk for a phase transition. This is not surprising given that the sample is from a general population sample. To compare, we calculated the bimodality coefficient (BC), which uses a function of the skewness and kurtosis from the distribution of the time series of the proportion of symptoms (see Hosenfeld et al. (2015) for more details). The BC obtains values between 0 and 1 and considers values > 0.55 to mean that there is evidence for two states. The BC classified 36.4% of the participants as being bimodal. When we compare the results from the MFA to the BC, we see that the methods agree in 75.4%.

Discussion

The present study combined dynamical systems theory and network theory to assess the risk for a phase transition, a sudden jump between two stable mood states, using a mean field

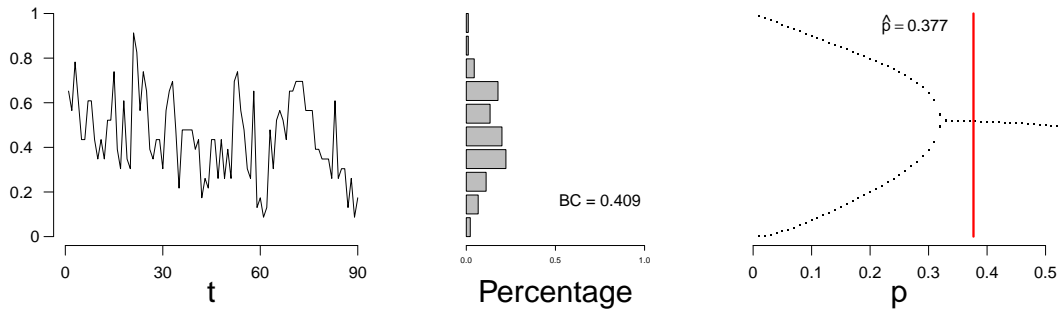


Figure 8. : Proportion of active symptoms (left) and bifurcation diagram (right) of one participant from the HowNutsAreTheDutch data. Red line indicates the estimation of \hat{p} .

approximation. We provided a simulation study and a validation that both show that a mean field approximation can accurately categorize individuals as having an increased risk for a phase transition or not. We then applied the mean field approximation to two different empirical examples: data from patients admitted to a closed ward, and data from a general sample from a nation-wide study. Results from these applications show how our proposed method works in practice.

Results showed that the majority of the clinical sample were categorized as having an increased risk for a phase transition. This indicates that these patients are likely to transition from a stable depressed mood state to a stable healthy mood state. Although we do not have any follow-up measures to investigate whether or not these phase transition actually occurred, we do know that these patients were eventually released from the closed ward. This may be an indication of that phase transition occurring in these patients. At the same time, the majority of the healthy sample were categorized as not having an increased risk for a phase transition. This indicates that these participants will probably not transition from the stable state that they are currently in. As the analyses that we ran are of a probabilistic nature, we cannot know whether or not participants actually experienced a phase transition. It would be interesting for future research to run the HowNutsAreTheDutch study again for those participants that were categorized as having an increased risk for a phase transition, and to investigate whether or not they received a clinical diagnosis.

When collecting time-series data, participants are requested multiple times a day to fill out a questionnaire for a certain period. This type of data collection demands time and energy of the participants. It thus makes sense that participants sometimes forget to complete a questionnaire, or are simply not up for it at that specific moment, for whatever reason. In the data that we analysed, we came across different ratio's of missing data and completed measurements, ranging from no missing measurements to almost as much as 90%. In this study we assumed a Markov model and so, the item responses should not change much and thus, we replaced missing measurements with the previous measurement. Adopting this approach for handling missing data decreases the variance that individual items may have, thereby increasing the probability that a participant is categorized as having an increased risk for a phase transition. Although we did not find evidence that our analysis differed much if we removed these measurements altogether, at

this point in time, there is no clear picture of the effects of missing data in time-series analyses. Future research should focus on mapping the effects that different types of missing data have on time-series analysis, and what the effect of various imputation methods have on the analyses.

The current study only allows for dichotomous, non-missing data. We applied different techniques for dichotomizing the data and handling missing data. Even though these different approaches did not lead to different conclusions, the current approach may not be ideal. Data are often imperfect: low variance within item scores, as well as missing data occurs recurrently in time-series data. More importantly, it can be argued that MDD symptoms may not be binary, but categorical or even continuous. One can imagine that there exists a scale on which individual MDD symptoms lie. For example, two participants may experience insomnia (one of the MDD symptoms as listed in the Diagnostic and Statistical Manual of Mental Disorders (American Psychiatric Association, 2013)), but the severity of this symptom may differ greatly between individuals. In the future we aim to expand the mean field approximation so that it allows continuous data as well as items with low variance.

In conclusion, this study supports the notion that we are able to assess an individual's risk for a phase transition before it may occur. In addition, the approach that we took in this study could aid clinical therapists by giving extra information about the risk that a patient may have in experiencing a phase transition. Furthermore, patients that have recovered from MDD can potentially be assisted by monitoring their risk for a relapse in MDD. Finally, this study has grounded psychopathology more firmly in dynamical systems theory, by providing a general mechanism, and in network theory, by describing under which circumstances we are able to use the mean field approximation.

Acknowledgements

This research was supported by European Research Council Consolidator Grant no. 647209.

JK is partly funded by the Research Priority Area Yield, part of the Research Institute of Child Development and Education, University of Amsterdam, the Netherlands.

The single-case experiment was designed by Prof. Dr. Marieke Wichers and Prof. Dr. Peter Groot. This study was supported by an Aspasia grant (MW., NWO grant), and by the Brain Foundation of the Netherlands (MW., grant No. F2012(1)-03).

The work on the HowNutsAreTheDutch project was supported by the Netherlands Organization for Scientific Research (NWO-ZonMW), by a VICI grant entitled Deconstructing Depression (no: 91812607) received by Prof. Dr. Peter de Jonge. Part of the HowNutsAreTheDutch project was realized in collaboration with the Espria Academy.

We thank Prof. Dr. Marieke Wichers and the HowNutsAreTheDutch project for letting us use their data. We also want to express our gratitude to Peter Groot, all the participants of the HowNutsAreTheDutch project, and the patients of the closed ward. The authors thank Prof. Dr. Marieke Wichers, Pia Tio and Dr. Maarten Marsman for their contributions to the manuscript.

References

- American Psychiatric Association. (2013). *Diagnostic and statistical manual of mental disorders (DSM-5{®})*. American Psychiatric Pub.
- Balister, P., Bollobás, B., & Kozma, R. (2006). Large deviations for mean field models of probabilistic cellular automata. *Random Structures & Algorithms*, 29, 399–415.
- Bollobás, B. (2001). *Random Graphs*. Cambridge, UK: Cambridge University Press.
- Borsboom, D., Cramer, A. O. J., Schmittmann, V. D., Epskamp, S., & Waldorp, L. J. (2011). The small world of psychopathology. *PloS one*, 6(11), e27407.
- Cramer, A. O. J., Sluis, S., Noordhof, A., Wichers, M., Geschwind, N., Aggen, S. H., ... Borsboom, D. (2012). Dimensions of normal personality as networks in search of equilibrium: You can't like parties if you don't like people. *European Journal of Personality*, 26, 414–431.
- Cramer, A. O. J., van Borkulo, C. D., Giltay, E. J., van der Maas, H. L. J., Kendler, K. S., Scheffer, M., & Borsboom, D. (2016). Major depression as a complex dynamical system. *PloS one*.
- Csikszentmihalyi, M., & Larson, R. (1987). Validity and reliability of the experience-sampling method. *The Journal of Nervous and Mental Disease*, 175, 137–193.
- Durett, R. (2007). *Random Graph Dynamics*. Cambridge, UK: Cambridge University Press.
- Epskamp, S. (2015). *IsingSampler: Sampling Methods and Distribution Functions for the Ising Model*. Retrieved from <https://cran.r-project.org/package=IsingSampler>
- Fleming, T. R., & Harrington, D. P. (1978). Estimation for discrete time nonhomogeneous Markov chains. *Stochastic Processes and their Applications*, 7, 131–139.
- Gordijn, M., Beersma, D., Bouhuys, A., Reinink, E., & van den Hoofdakker, R. (1994). A longitudinal study of diurnal mood variation in depression: characteristics and significance. *Journal of Affective Disorders*, 31, 261–273.
- Gordijn, M., Beersma, D., Bouhuys, A., & van den Hoofdakker, R. (1998). Mood variability and sleep deprivation effect as predictors of therapeutic response in depression. *Sleep-wake research in the Netherlands*, 9, 41–44.
- Guloksuz, S., Pries, L. K., & Van Os, J. (2017). Application of network methods for understanding mental disorders: pitfalls and promise. *Psychological medicine*, 47(16), 2743–2752.
- Gulyás, L., Kampis, G., & Legendi, R. O. (2013). Elementary models of dynamic networks. *The European Physical Journal Special Topics*, 222(6), 1311–1333.
- Hirsch, M. W., Smale, S., & Devaney, R. L. (2012). *Differential equations, dynamical systems, and an introduction to chaos*. Academic press.
- Hosenfeld, B., Bos, E. H., Wardenaar, K. J., Conradi, H. J., van der Maas, H. L. J., Visser, I., & de Jonge, P. (2015). Major depressive disorder as a nonlinear dynamic system: bimodality in the frequency distribution of depressive symptoms over time. *BMC Psychiatry*, 15, 1–9.
- Kossakowski, J. J. (2018). *Results from "The Introduction of the Mean Field Approximation to Psychology: Combining Dynamical Systems Theory and Network Theory in Major Depressive Disorder"*. Retrieved from <https://osf.io/edyzp/>.
- Kossakowski, J. J., & Cramer, A. O. J. (2018). Complexity, chaos and catastrophe: Modeling psychopathology as a dynamic system. In *Frontiers of cognitive psychology* (chap. Network Sc).
- Kossakowski, J. J., Groot, P. C., Haslbeck, J. M. B., Borsboom, D., & Wichers, M. (2017). Data from 'Critical Slowing Down as a Personalized Early Warning Signal for Depression'. *Journal of Open Psychology Data*, 5, 1–3.
- Kozma, R., Puljic, M., Balister, P., Bollobás, B., & Freeman, W. J. (2004). Neuropercolation: a random cellular automata approach to spatio-temporal neurodynamics. In *Cellular automata* (pp. 435–443). Springer.
- Kozma, R., Puljic, M., Balister, P., Bollobás, B., & Freeman, W. J. (2005). Phase transitions in the neuropercolation model of neural populations with mixed local and non-local interactions. *Biological*

- Cybernetics*, 92, 367–379.
- Kuznetsov, Y. A. (2013). *Elements of applied bifurcation theory*. New York, USA: Springer-Verlag.
- Lebowitz, J. L., Maes, C., & Speer, E. R. (1990). Statistical mechanics of probabilistic cellular automata. *Journal of Statistical Physics*, 59, 117–170.
- Newman, M. E. J., & Watts, D. J. (1999). Renormalization group analysis of the small-world network model. *Physics Letters A*, 263, 4–6.
- R Core Team. (2016). *R: A Language and Environment for Statistical Computing*. Vienna, Austria: R Foundation for Statistical Computing. Retrieved from <https://www.r-project.org/>
- Rajarshi, M. B. (2012). *Statistical Inference for Discrete Time Stochastic Processes*. Springer.
- Sarkar, P. (2000). A brief history of cellular automata. *ACM Computing Surveys (CSUR)*, 32(1), 80–107.
- Scheffer, M., Bascompte, J., Brock, W. A., Brovkin, V., Carpenter, S. R., Dakos, V., ... Sugihara, G. (2014). Early-warning signals for critical transitions. *Nature*, 46, 53–59.
- van de Leemput, I. A., Wicher, M., Cramer, A. O. J., Borsboom, D., Tuerlinckx, F., Kuppens, P., ... Scheffer, M. (2014). Critical Slowing Down as Early Warning for the Onset and Termination of Depression. *Proceedings of the National Academy of Sciences*, 111, 87–92.
- van der Krieke, L., Jeronimus, B. F., Blaauw, F. J., Wanders, R. B. K., Emerencia, A. C., Schenk, H. M., ... de Jonge, P. (2015). HowNutsAreTheDutch (HoeGekIsNL): A crowdsourcing study of mental symptoms and strengths. *International Journal of Methods in Psychiatric Research*, 25, 123–144.
- von Zerssen, D. (1986). Clinical self-rating scales (CSRS) of the Munich psychiatric information system (PSYCHIS M{ü}nchen). In *Assessment of depression* (pp. 270–303). Springer.
- Waldorp, L. J., & Kossakowski, J. J. (2018). *Mean Field Dynamics of Graphs I: Evolution of Probabilistic Cellular Automata on Different Types of Graphs*. In preparation.
- Watts, D. J., & Strogatz, S. H. (1998). Collective dynamics of small-world' networks. *Nature*, 393, 440–442.
- Wichers, M., Groot, P. C., Psychosystems, ESM Group, & ESW Group. (2016). Critical Slowing Down as a Personalized Early Warning Signal for Depression. *Psychotherapy and Psychosomatics*, 85, 114–116.
- Wolfram, S. (1984). Computation theory of cellular automata. *Communications in Mathematical Physics*, 96(1), 15–57.
- World Health Organization. (2012). *Depression, a hidden burden*. Retrieved from: <http://www.who.int>.